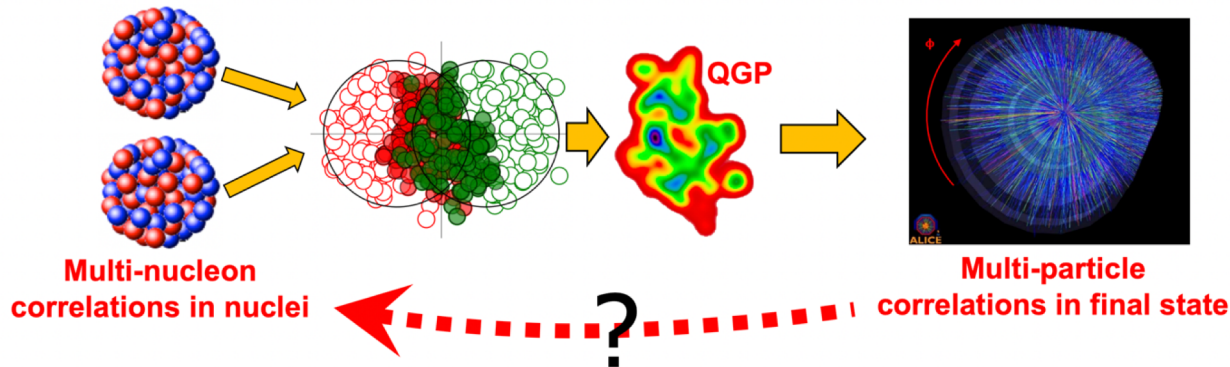


原子核结构与相对论重离子碰撞前沿交叉研讨会

Nuclear shape imaging in heavy ion collisions

Jiangyong Jia

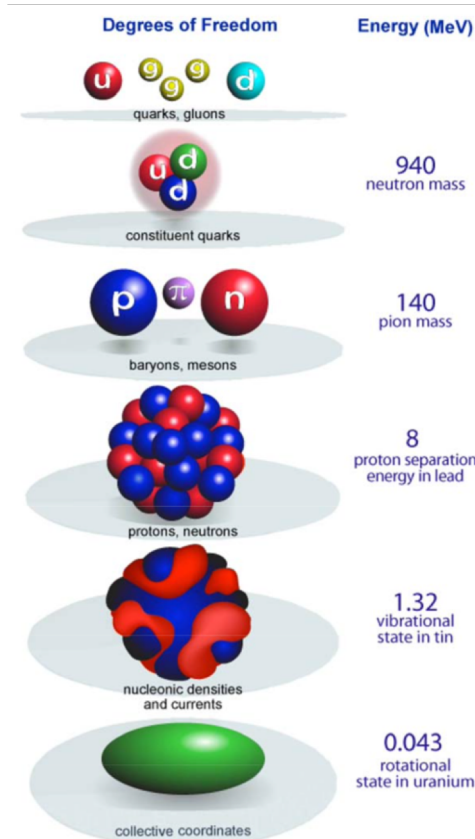


Stony Brook University

July 31-August 6, 2023

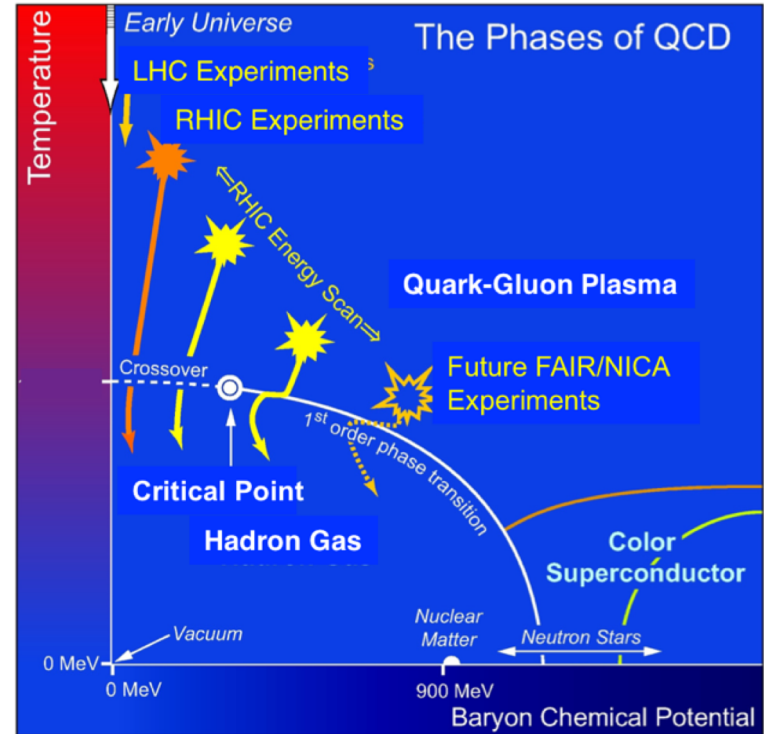
Landscape of nuclear physics

Quark-gluon plasma



hadrons

nuclei

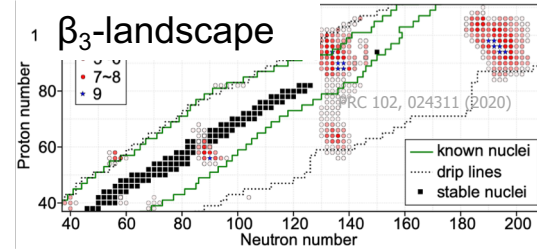
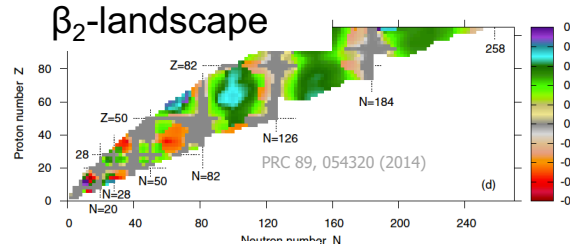
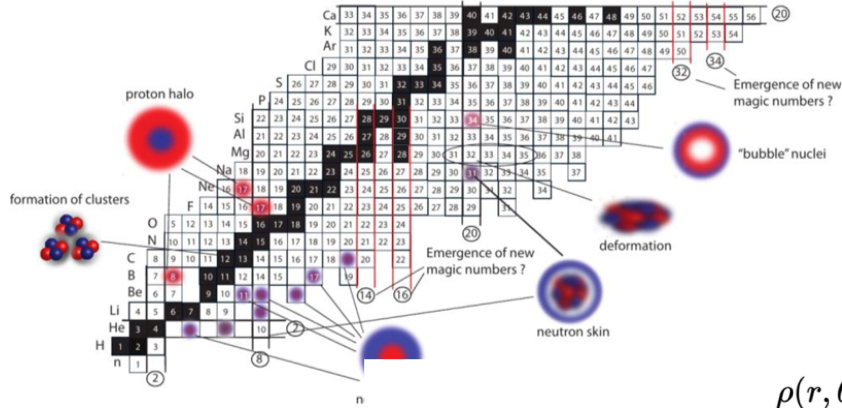


Most nuclear experiments starts with nuclei

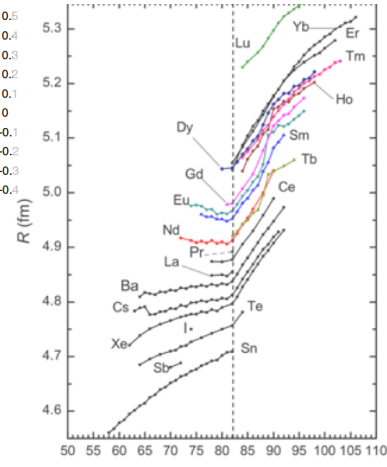
Collective structure of atomic nuclei

Emergent phenomena of the many-body quantum system

- clustering, halo, skin, bubble...
- quadrupole/octupole/hexadecapole deformations
- Non-monotonic evolution with N and Z

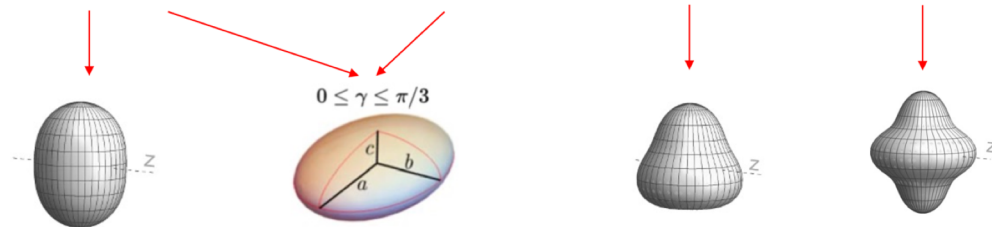
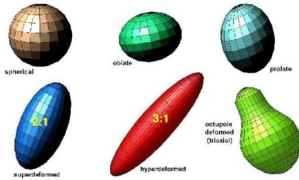


Radii-landscape

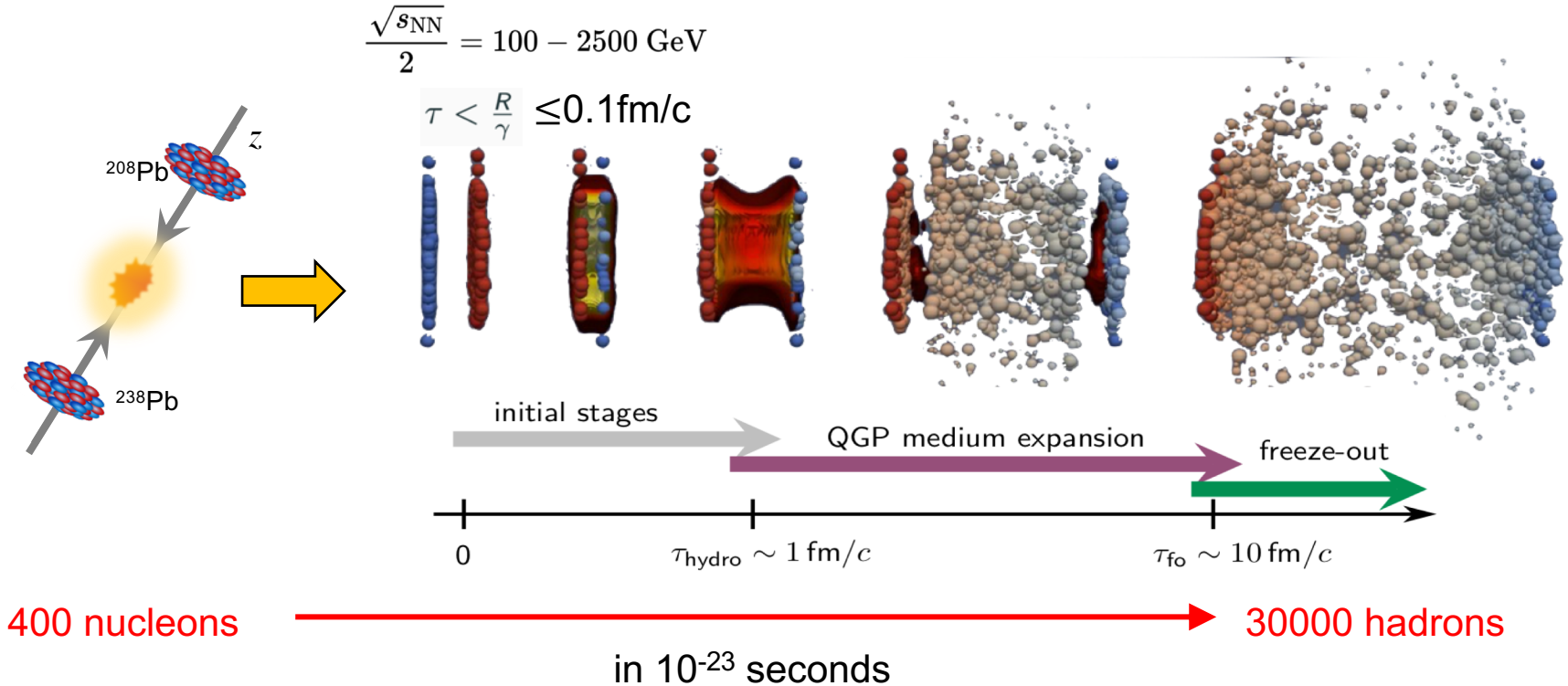


$$\rho(r, \theta, \phi) = \frac{\rho_0}{1 + e^{(r-R(\theta, \phi))/a_0}}$$

$$R(\theta, \phi) = R_0(1 + \beta_2[\cos \gamma Y_{2,0}(\theta, \phi) + \sin \gamma Y_{2,2}(\theta, \phi)] + \beta_3 Y_{3,0}(\theta, \phi) + \beta_4 Y_{4,0}(\theta, \phi))$$



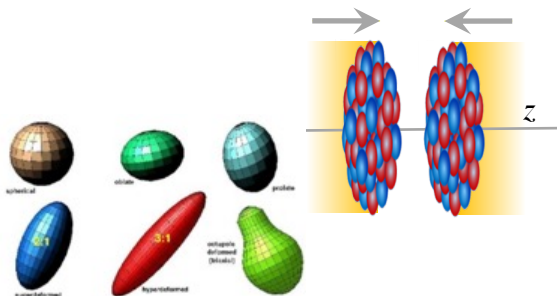
High-energy heavy ion collision



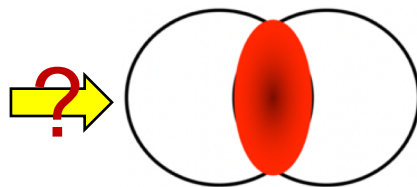
- 1) Extremely short passing time to take a snap-shot of the nuclear wavefunction in the two nuclei.
- 2) Large particle production in overlap region means QGP is dense and expand hydrodynamically.

Collective flow assisted nuclear structure imaging

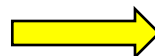
Nuclear structure



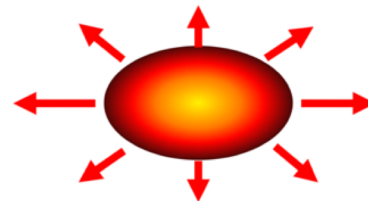
Initial condition



hydrodynamics



Final state



Shape and radial dis.

- $\beta_2 \rightarrow$ Quadrupole deformation
- $\beta_3 \rightarrow$ Octupole deformation
- $a_0 \rightarrow$ Surface diffuseness
- $R_0 \rightarrow$ Nuclear size

Volume, size and shape

$$N_{\text{part}}$$

$$R_{\perp}^2 \propto \langle r_{\perp}^2 \rangle$$

$$\mathcal{E}_n \propto \langle r_{\perp}^n e^{in\phi} \rangle$$

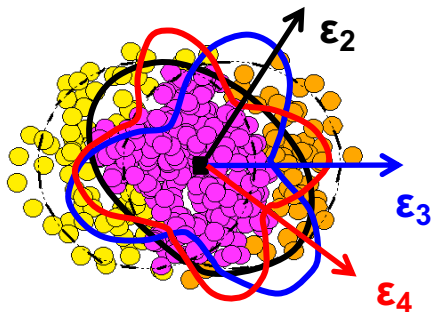
Observables

$$\frac{d^2 N}{d\phi dp_T} = N(p_T) \left(\sum_n V_n e^{-in\phi} \right)$$

- **Constrain the initial condition** by comparing nuclei with known structure properties
- **Reveal novel properties of nuclei** by leveraging known hydrodynamic response.

Infer initial condition from flow correlations

Initial state shape



volume, size and shape

$$N_{\text{part}} \quad R_{\perp}^2 \propto \langle r_{\perp}^2 \rangle, \quad \mathcal{E}_2 \propto \langle r_{\perp}^2 e^{i2\phi} \rangle$$

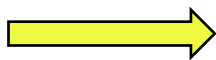
$$\mathcal{E}_3 \propto \langle r_{\perp}^3 e^{i3\phi} \rangle$$

$$\mathcal{E}_4 \propto \langle r_{\perp}^4 e^{i4\phi} \rangle$$

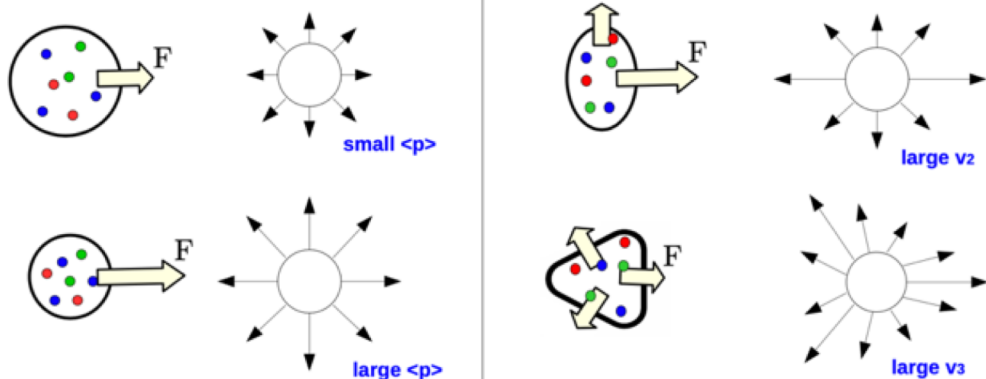
...

$$F = -\nabla P(\epsilon)$$

Hydro-response



Final state flow



Multiplicity

Radial Flow

Harmonic Flow

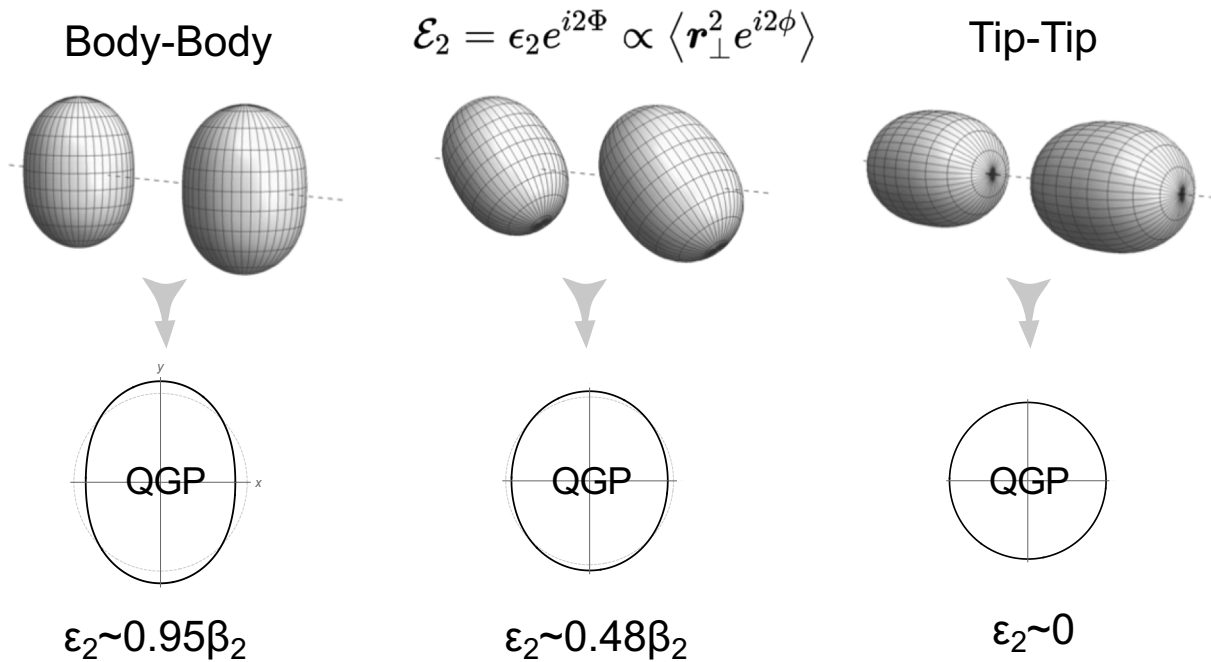
N_{ch}

$$\frac{d^2 N}{d\phi dp_T} = N(p_T) \left(\sum_n V_n e^{-in\phi} \right) \quad 1206.1905$$

Flow-assisted imaging relies on linear response:

$$N_{\text{ch}} \propto N_{\text{part}} \quad \frac{\delta[p_T]}{[p_T]} \propto -\frac{\delta R_{\perp}}{R_{\perp}} \quad V_n \propto \mathcal{E}_n$$

Connecting initial condition to nuclear shape



$$\epsilon_2 = \underbrace{\epsilon_0}_{\text{undeformed}} + \underbrace{p(\Omega_1, \Omega_2)}_{\text{phase factor}} \beta_2 + \mathcal{O}(\beta_2^2)$$

Shape depends on Euler angle $\Omega = \phi\theta\psi$



$$\langle \epsilon_2^2 \rangle \approx \langle \epsilon_0^2 \rangle + 0.2\beta_2^2$$

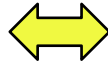
$$\langle v_n^2 \rangle \propto \langle \epsilon_n^2 \rangle \quad \text{In intrinsic frame}$$

Impact of nuclear shape on many-body correlations

$$\rho(r, \theta, \phi) = \frac{\rho_0}{1 + e^{(r-R(\theta, \phi))/a_0}} \quad R(\theta, \phi) = R_0(1 + \beta_2[\cos \gamma Y_{2,0}(\theta, \phi) + \sin \gamma Y_{2,2}(\theta, \phi)] + \beta_3 Y_{3,0}(\theta, \phi) + \beta_4 Y_{4,0}(\theta, \phi))$$

- In principle, can probe any moments of $p(1/R, \varepsilon_2, \varepsilon_3 \dots)$ via $p([p_T], v_2, v_3 \dots)$...

| | | |
|-------------|--|--|
| ■ Mean | $\langle d_\perp \rangle$ $d_\perp \equiv 1/R_\perp$ | $\langle p_T \rangle$ |
| ■ Variance: | $\langle \varepsilon_n^2 \rangle, \langle (\delta d_\perp / d_\perp)^2 \rangle$ | $\langle v_n^2 \rangle, \langle (\delta p_T / p_T)^2 \rangle$ |
| ■ Skewness | $\langle \varepsilon_n^2 \delta d_\perp / d_\perp \rangle, \langle (\delta d_\perp / d_\perp)^3 \rangle$ | $\langle v_n^2 \delta p_T / p_T \rangle, \langle (\delta p_T / p_T)^3 \rangle$ |
| ■ Kurtosis | $\langle \varepsilon_n^4 \rangle - 2\langle \varepsilon_n^2 \rangle^2, \langle (\delta d_\perp / d_\perp)^4 \rangle - 3\langle (\delta d_\perp / d_\perp)^2 \rangle^2$ | $\langle v_n^4 \rangle - 2\langle v_n^2 \rangle^2, \langle (\delta p_T / p_T)^4 \rangle - 3\langle (\delta p_T / p_T)^2 \rangle^2$ |
| ... | | |



Impact of nuclear shape on many-body correlations

$$\rho(r, \theta, \phi) = \frac{\rho_0}{1 + e^{(r-R(\theta, \phi))/a_0}} \quad R(\theta, \phi) = R_0(1 + \beta_2[\cos \gamma Y_{2,0}(\theta, \phi) + \sin \gamma Y_{2,2}(\theta, \phi)] + \beta_3 Y_{3,0}(\theta, \phi) + \beta_4 Y_{4,0}(\theta, \phi))$$

- In principle, can probe any moments of $p(1/R, \varepsilon_2, \varepsilon_3 \dots)$ via $p([p_T], v_2, v_3 \dots)$...

| | | | |
|-------------|--|--|--|
| ■ Mean | $\langle d_\perp \rangle$ | $d_\perp \equiv 1/R_\perp$ | $\langle p_T \rangle$ |
| ■ Variance: | $\langle \varepsilon_n^2 \rangle$ | $\langle (\delta d_\perp / d_\perp)^2 \rangle$ | $\langle v_n^2 \rangle, \langle (\delta p_T / p_T)^2 \rangle$ |
| ■ Skewness | $\langle \varepsilon_n^2 \delta d_\perp / d_\perp \rangle$ | $\langle (\delta d_\perp / d_\perp)^3 \rangle$ | $\langle v_n^2 \delta p_T / p_T \rangle, \langle (\delta p_T / p_T)^3 \rangle$ |
| ■ Kurtosis | $\langle \varepsilon_n^4 \rangle - 2\langle \varepsilon_n^2 \rangle^2$ | $\langle (\delta d_\perp / d_\perp)^4 \rangle - 3\langle (\delta d_\perp / d_\perp)^2 \rangle^2$ | $\langle v_n^4 \rangle - 2\langle v_n^2 \rangle^2, \langle (\delta p_T / p_T)^4 \rangle - 3\langle (\delta p_T / p_T)^2 \rangle^2$ |



...

- All have a simple connection to deformation:

- Variances

$$\langle \varepsilon_2^2 \rangle \sim a_2 + b_2 \beta_2^2 + \underline{b_{2,3} \beta_3^2}$$

$$\langle \varepsilon_3^2 \rangle \sim a_3 + b_3 \beta_3^2$$

$$\langle \varepsilon_4^2 \rangle \sim a_4 + b_4 \beta_4^2$$

$$\langle (\delta d_\perp / d_\perp)^2 \rangle \sim a_0 + b_0 \beta_2^2 + b_{0,3} \beta_3^2$$

- Skewness

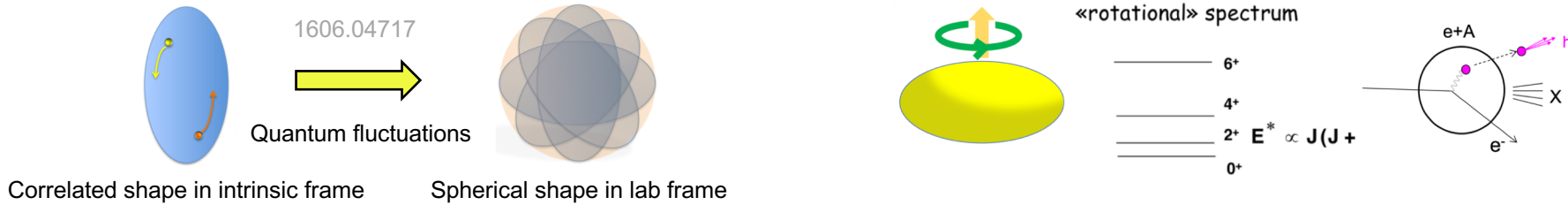
$$\langle \varepsilon_2^2 \delta d_\perp / d_\perp \rangle \sim a_1 - b_1 \cos(3\gamma) \beta_2^3$$

$$\langle (\delta d_\perp / d_\perp)^3 \rangle \sim a_2 + b_2 \cos(3\gamma) \beta_2^3$$

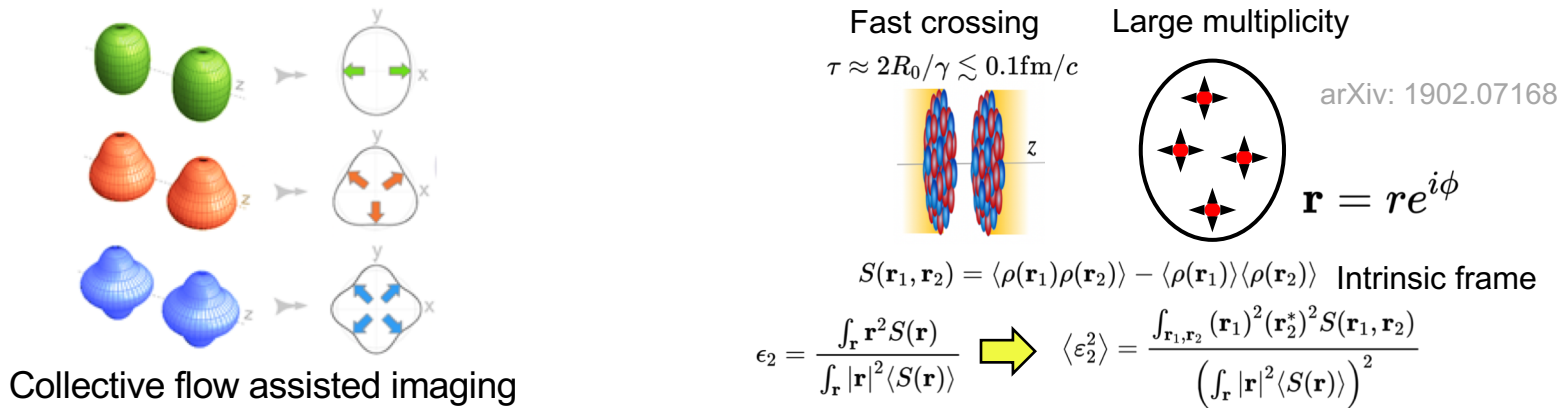
.....

Low-energy vs high-energy method

- Intrinsic frame shape not directly visible in lab frame at time scale $\tau > I/\hbar \sim 10^{-21}$ s
- Mainly inferred from non-invasive spectroscopy methods.



- High-energy collisions destructive imaging: probe entire mass distribution in the intrinsic frame via multi-point correlations. Shape frozen in nuclear crossing (10^{-24} s \ll rotational time scale 10^{-21} s)



Analogy: Coulomb Explosion Imaging

Instantaneous stripping of electrons (thin foil or x-ray laser), and then let atoms explode under mutual coulomb repulsion

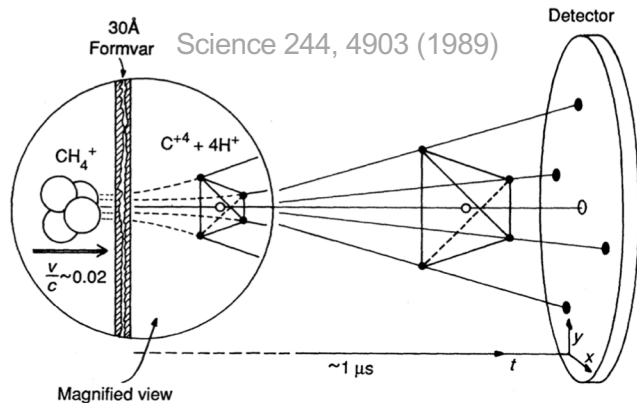
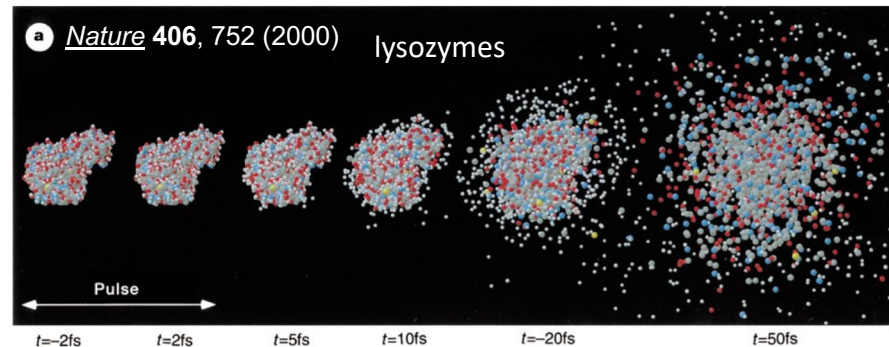
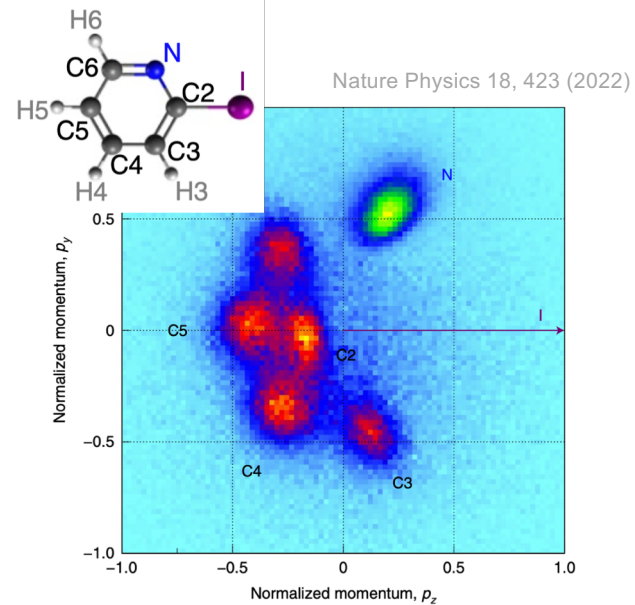


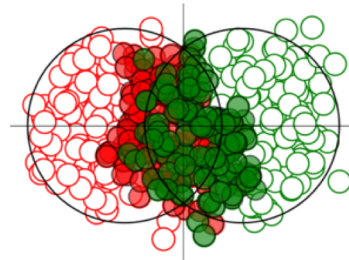
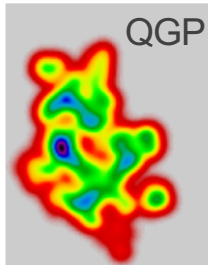
Fig. 1. A schematic view of a Coulomb explosion experiment. When a swift molecule passes through a thin solid film, it loses all of its binding electrons. The remaining positive ions repel each other, thus transforming the microstructure (as seen in the magnified view) into a macrostructure that can be measured precisely with an appropriate detector. The measured traces (x , y , t) of each fragment nucleus for individual molecules are then transformed into the original molecular structure.



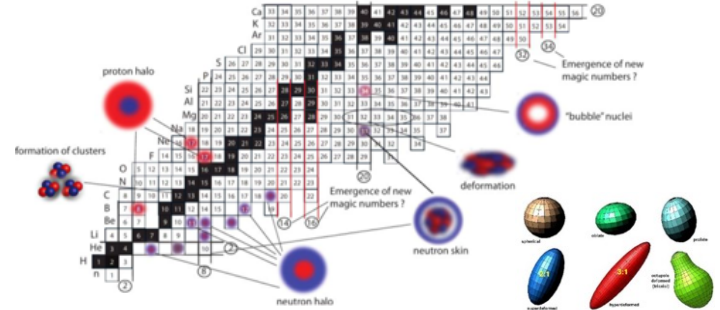
Strategy for nuclear shape imaging

Flow observable = $k \otimes$ initial condition (structure)

QGP response,
a smooth function of N+Z



Structure of colliding nuclei,
non-monotonic function of N and Z



Compare two systems of similar size but different structure

Isobar collisions at RHIC

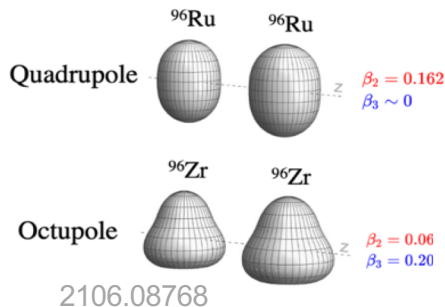
$^{96}\text{Ru}+^{96}\text{Ru}$ and $^{96}\text{Zr}+^{96}\text{Zr}$ at $\sqrt{s_{NN}}=200$ GeV

- A key question for any HI observable \mathcal{O} :

$$\frac{\mathcal{O}^{96}\text{Ru}+^{96}\text{Ru}}{\mathcal{O}^{96}\text{Zr}+^{96}\text{Zr}} \stackrel{?}{=} 1$$

Deviation from 1 must have an origin in the nuclear structure, which impacts the initial state and then survives to the final state.

- Expectation



$$\mathcal{O} \approx b_0 + b_1\beta_2^2 + b_2\beta_3^2 + b_3(R_0 - R_{0,\text{ref}}) + b_4(a - a_{\text{ref}})$$

2109.00131

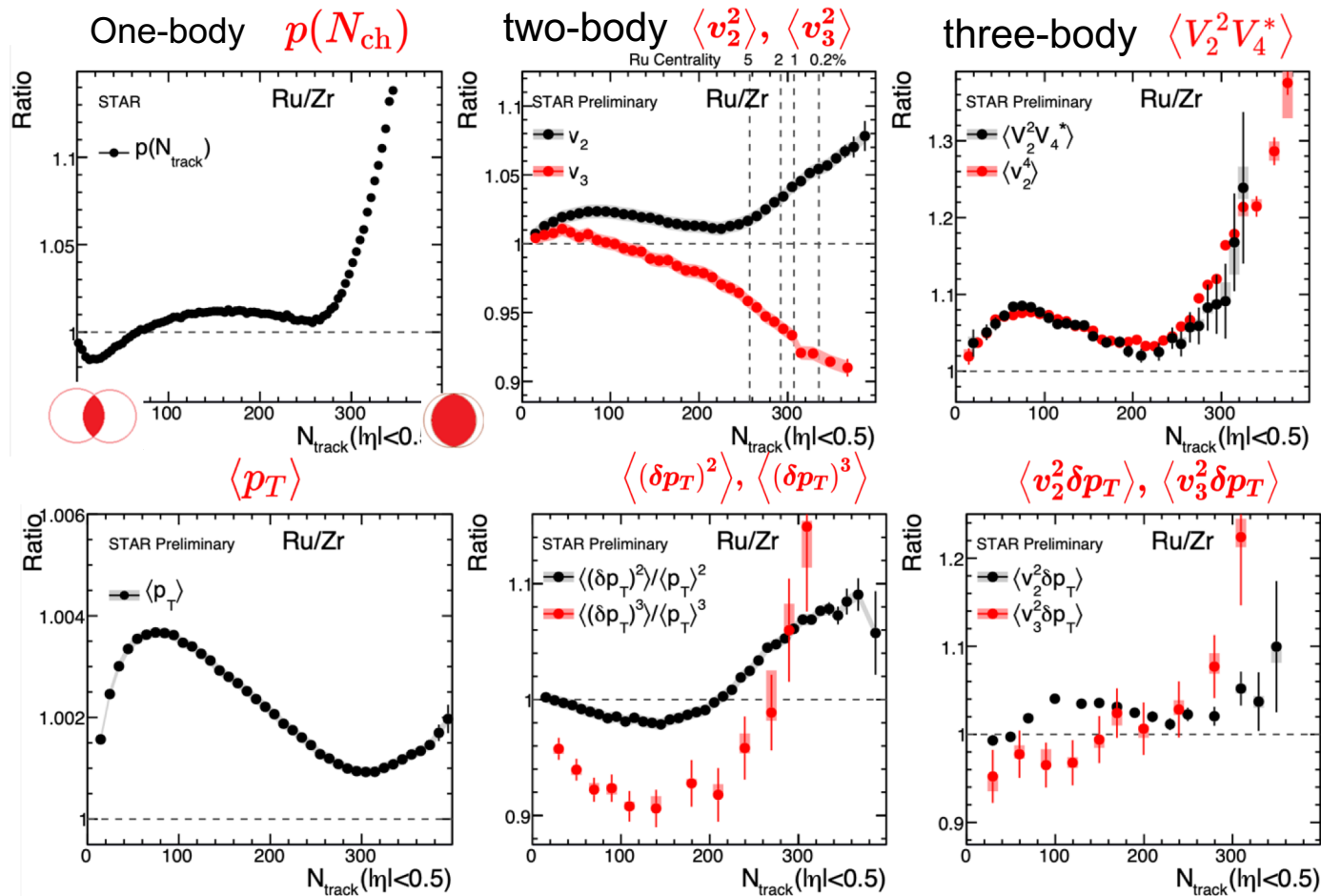
$$R_{\mathcal{O}} \equiv \frac{\mathcal{O}_{\text{Ru}}}{\mathcal{O}_{\text{Zr}}} \approx 1 + c_1\Delta\beta_2^2 + c_2\Delta\beta_3^2 + c_3\Delta R_0 + c_4\Delta a$$

Only probe structure differences

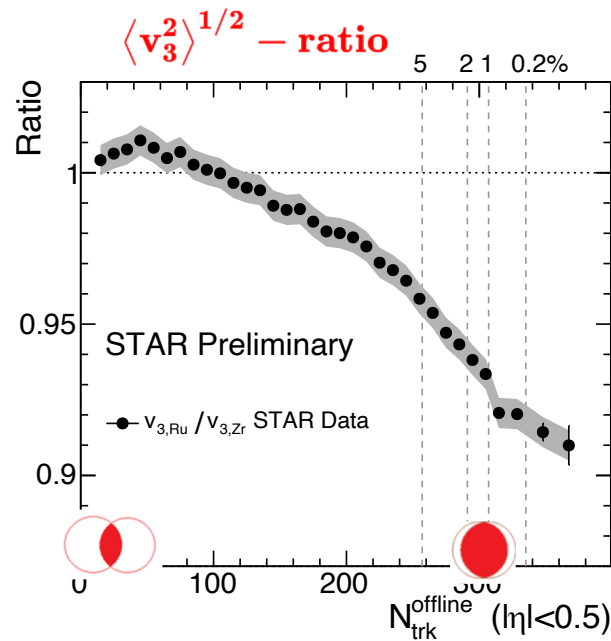
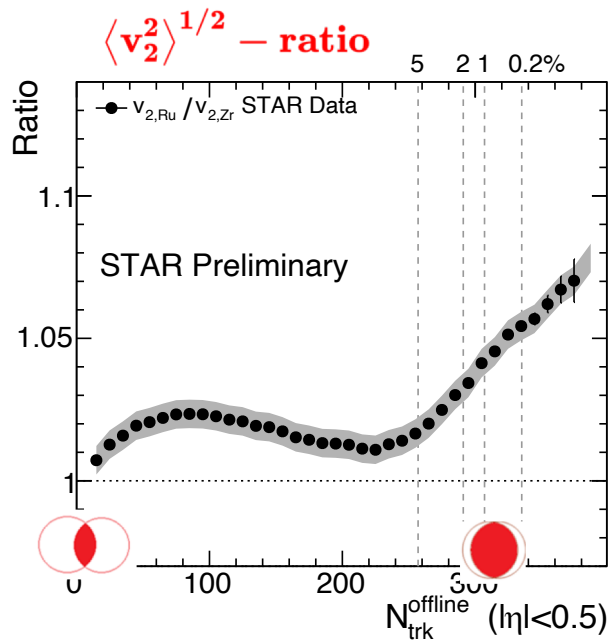
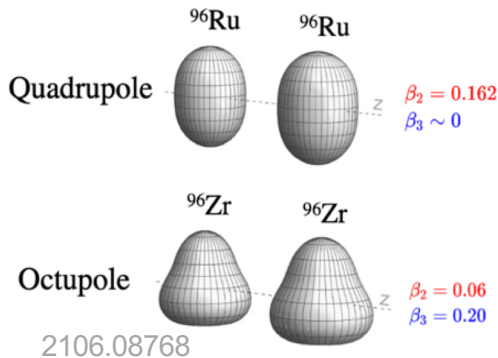
| Species | β_2 | β_3 | a_0 | R_0 |
|------------|-------------------|-------------------|--------------|--------------|
| Ru | 0.162 | 0 | 0.46 fm | 5.09 fm |
| Zr | 0.06 | 0.20 | 0.52 fm | 5.02 fm |
| difference | $\Delta\beta_2^2$ | $\Delta\beta_3^2$ | Δa_0 | ΔR_0 |
| | 0.0226 | -0.04 | -0.06 fm | 0.07 fm |

Structure influences everywhere

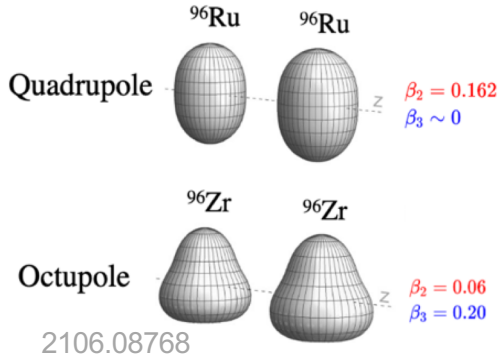
$$R_{\mathcal{O}} \equiv \frac{\mathcal{O}_{\text{Ru}}}{\mathcal{O}_{\text{Zr}}}$$



Nuclear structure via v_2 -ratio and v_3 -ratio



Nuclear structure via v_2 -ratio and v_3 -ratio



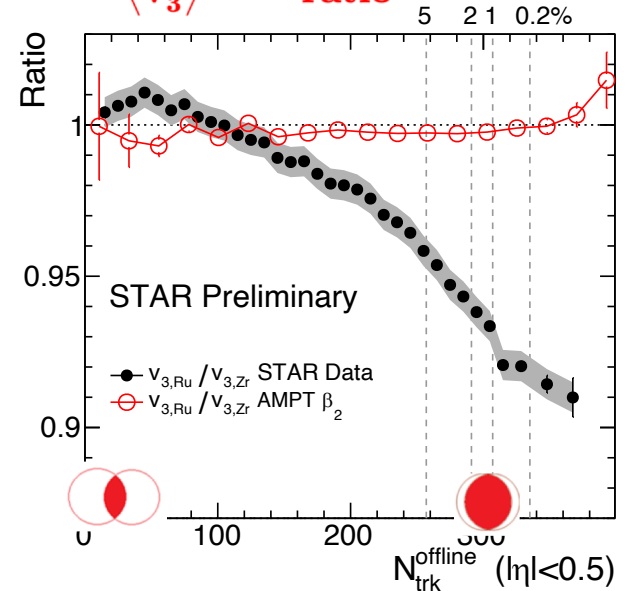
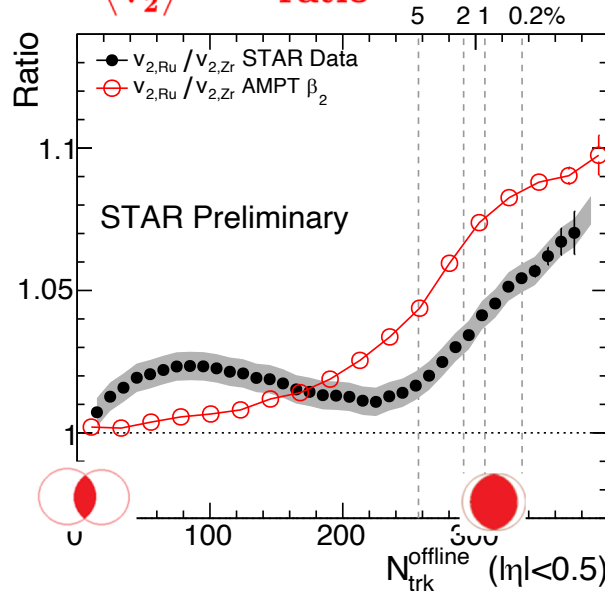
- $\beta_{2\text{Ru}} \sim 0.16$ increase v_2 , no influence on v_3 ratio

$$\langle v_2^2 \rangle \sim a_2 + b_2 \beta_2^2 + c_2 \beta_3^2$$

$$\langle v_3^2 \rangle \sim a_3 + b_3 \beta_3^2$$

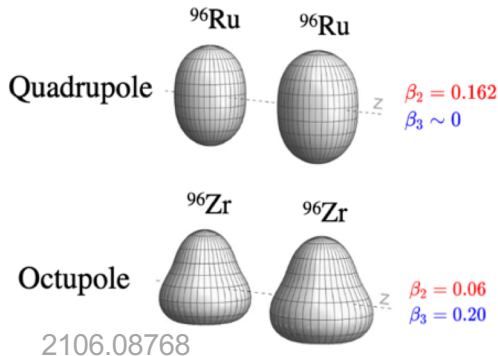
$\langle v_2^2 \rangle^{1/2}$ - ratio

$\langle v_3^2 \rangle^{1/2}$ - ratio



Compare with AMPT
-- a proxy for hydro

Nuclear structure via v_2 -ratio and v_3 -ratio



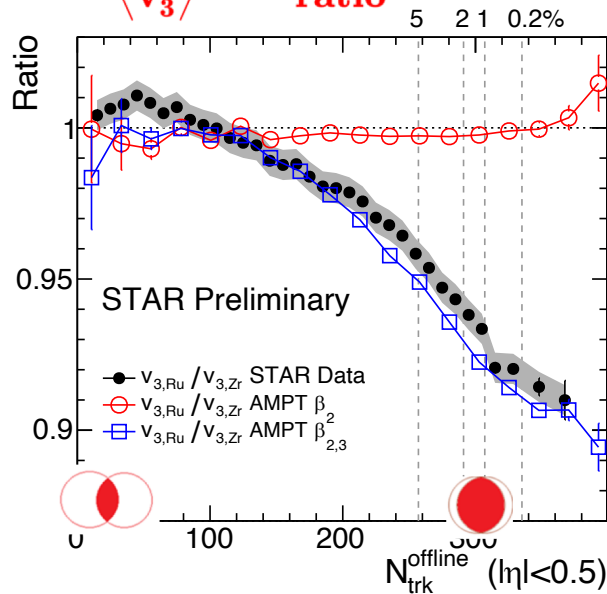
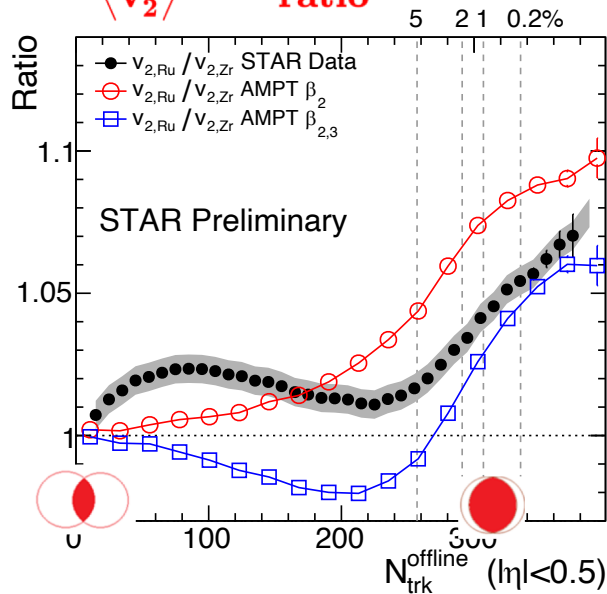
- $\beta_{2\text{Ru}} \sim 0.16$ increase v_2 , no influence on v_3 ratio
- $\beta_{3\text{Zr}} \sim 0.2$ decrease v_2 in mid-central, decrease v_3 ratio

$$\langle v_2^2 \rangle \sim a_2 + b_2 \beta_2^2 + c_2 \beta_3^2$$

$$\langle v_3^2 \rangle \sim a_3 + b_3 \beta_3^2$$

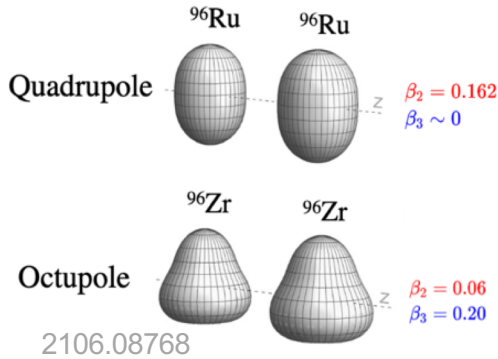
$\langle v_2^2 \rangle^{1/2}$ - ratio

$\langle v_3^2 \rangle^{1/2}$ - ratio



Compare with AMPT
-- a proxy for hydro

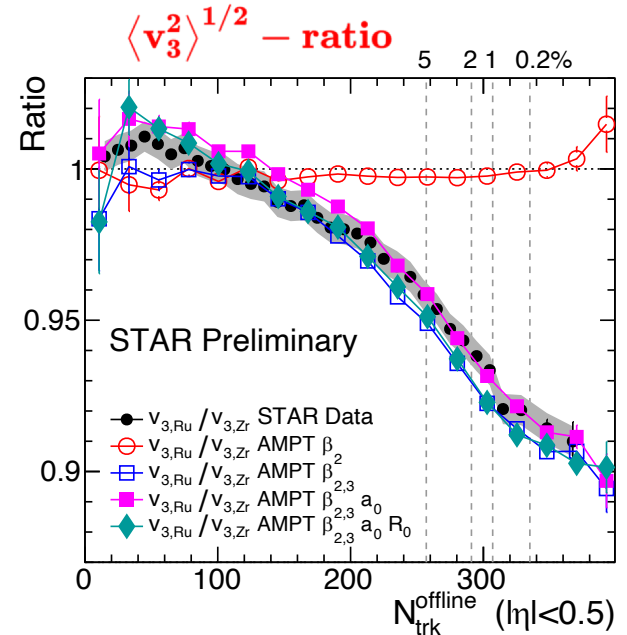
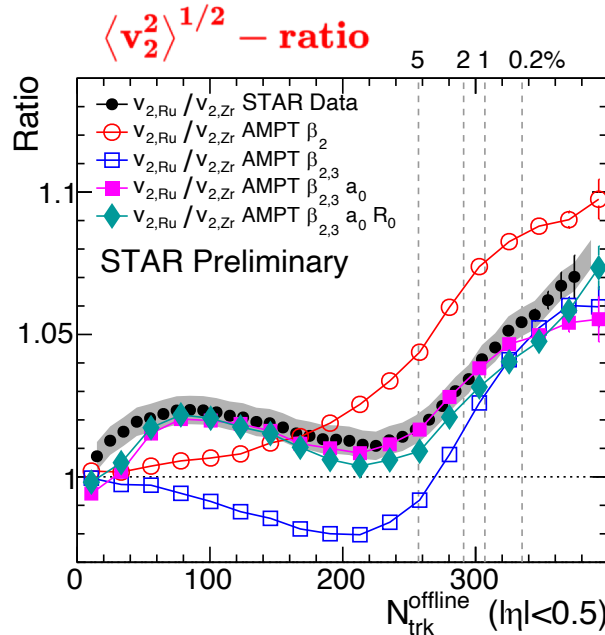
Nuclear structure via v_2 -ratio and v_3 -ratio



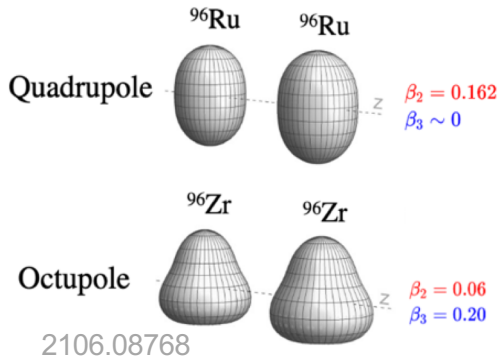
- $\beta_{2\text{Ru}} \sim 0.16$ increase v_2 , no influence on v_3 ratio
- $\beta_{3\text{Zr}} \sim 0.2$ decrease v_2 in mid-central, decrease v_3 ratio
- $\Delta a_0 = -0.06$ fm increase v_2 mid-central, small impact on v_3
- Radius $\Delta R_0 = 0.07$ fm only slightly affects v_2 and v_3 ratio.

Compare with AMPT
 -- a proxy for hydro

Sharper surface enhance v_2
 in mid-central collisions
 arXiv: 2206.10449



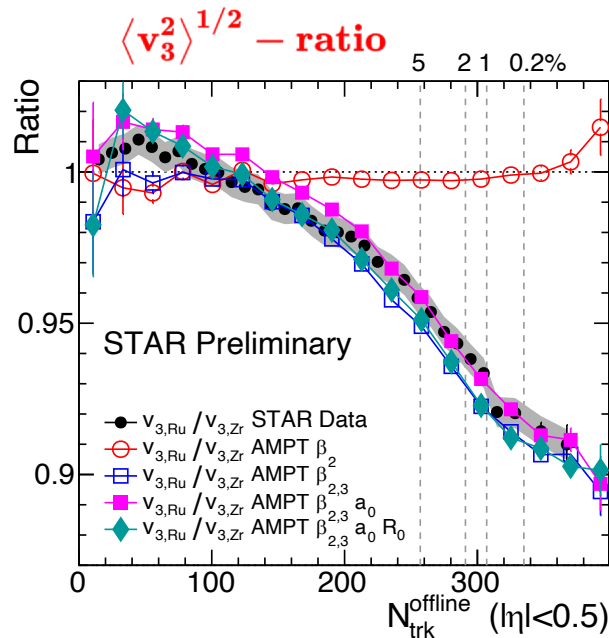
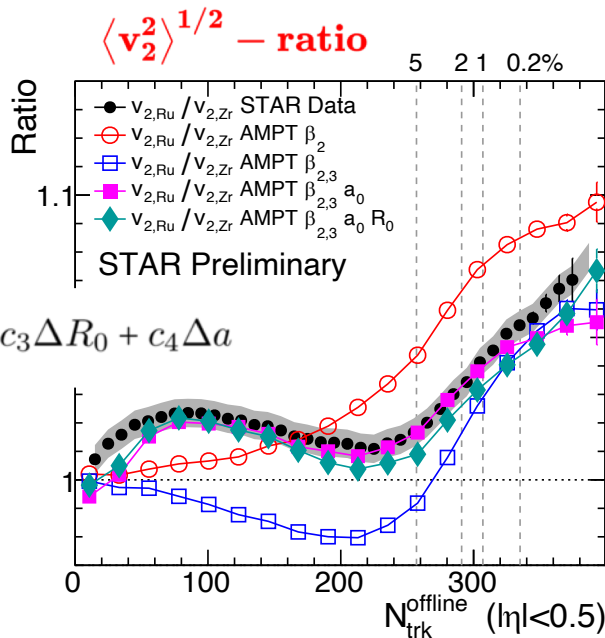
Nuclear structure via v_2 -ratio and v_3 -ratio



- $\beta_{2\text{Ru}} \sim 0.16$ increase v_2 , no influence on v_3 ratio
- $\beta_{3\text{Zr}} \sim 0.2$ decrease v_2 in mid-central, decrease v_3 ratio
- $\Delta a_0 = -0.06$ fm increase v_2 mid-central, small impact on v_3
- Radius $\Delta R_0 = 0.07$ fm only slightly affects v_2 and v_3 ratio.

$$R_{\mathcal{O}} \equiv \frac{O_{\text{Ru}}}{O_{\text{Zr}}} \approx 1 + c_1 \Delta \beta_2^2 + c_2 \Delta \beta_3^2 + c_3 \Delta R_0 + c_4 \Delta a$$

Simultaneously constrain
four structure parameters



Isobar ratios cancel final state effects

- Vary the shear viscosity by changing partonic cross-section in AMPT
 - Flow signal change by 30-50%, the v_n ratio unchanged.

$$v_n = k_n \varepsilon_n$$

↓

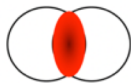
$$\frac{v_{n,Ru}}{v_{n,Zr}} \approx \frac{\varepsilon_{n,Ru}}{\varepsilon_{n,Zr}}$$

Robust probe of
initial state!

Nuclear structure

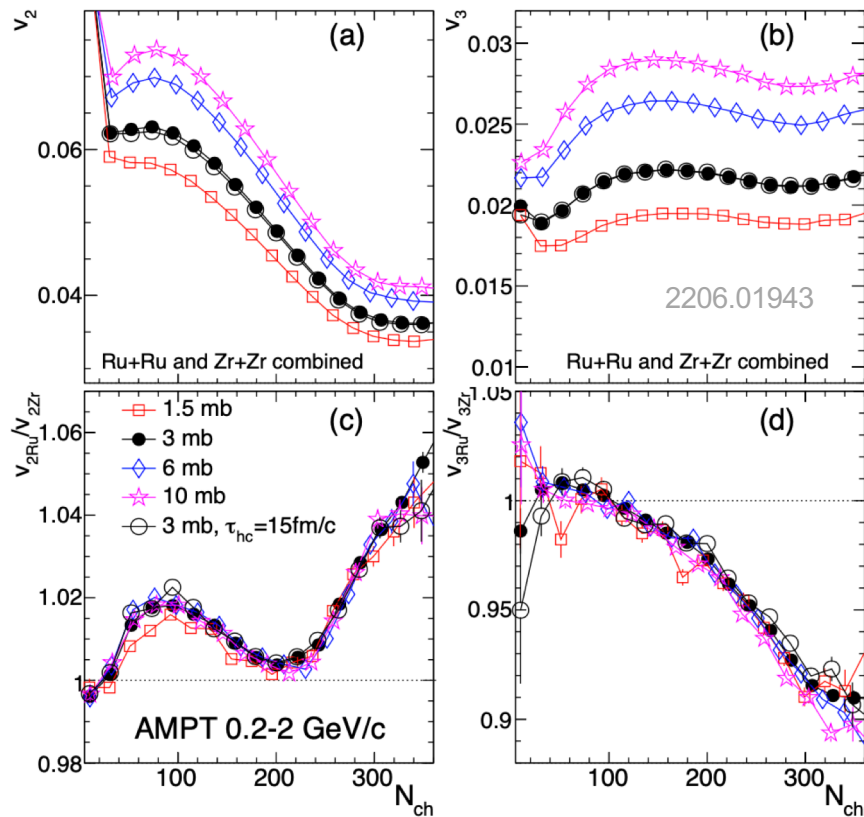


Initial condition



hydro

Final state

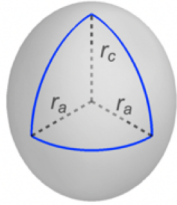


Triaxiality $R(\theta, \phi) = R_0 \left(1 + \beta_2 [\cos \gamma Y_{2,0} + \sin \gamma Y_{2,2}] \right)$

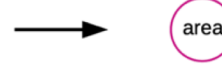
G. Giuliano et al 1910.04673, 2004.14463

Prolate

$$\beta_2 = 0.25, \cos(3\gamma) = 1$$



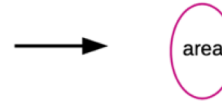
tip-tip



small v_2
small area
large $[p_T]$

$$v_2 \searrow \quad p_T \nearrow$$

body-body

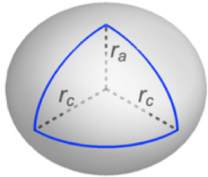


large v_2
large area
small $[p_T]$

$$v_2 \nearrow \quad p_T \searrow$$

Triaxial

$$\beta_2 = 0.25, \cos(3\gamma) = 0$$



Need 3-point correlators to probe the 3 axes

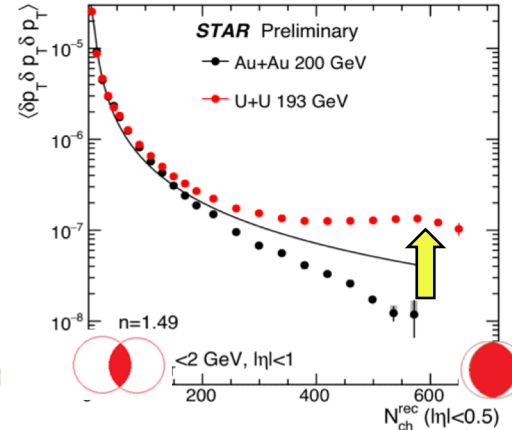
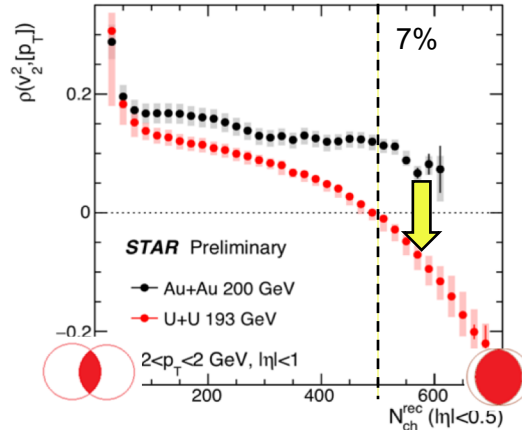
$$\langle v_2^2 \delta p_T \rangle \sim -\beta_2^3 \cos(3\gamma)$$

$$\langle (\delta p_T)^3 \rangle \sim \beta_2^3 \cos(3\gamma)$$

2109.00604

v_2 - $[p_T]$ covariance

$[p_T]$ skewness



Compare U+U vs Au+Au:

$$\beta_{2U} \sim 0.28, \beta_{2Au} \sim 0.13:$$

Extracting the ^{238}U deformation from STAR

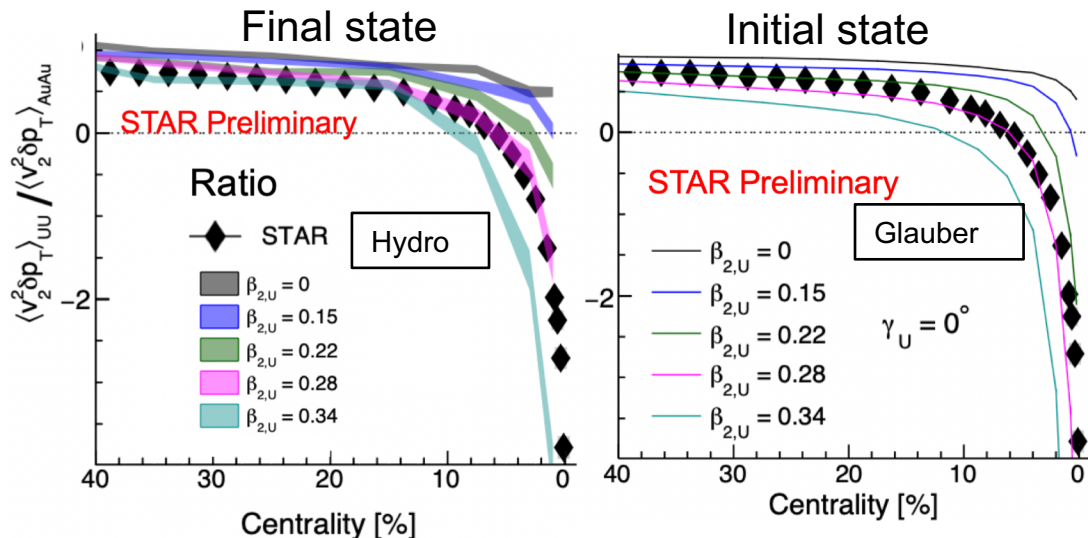
Take ratio of correlations to constrain $\beta_{2\text{U}}$

$$\frac{\langle v_2^2 \delta p_T \rangle_{\text{UU}}}{\langle v_2^2 \delta p_T \rangle_{\text{AuAu}}}$$

Compare with hydro and Glauber model
 \rightarrow clearly reflects initial state geometry

Derive Woods-Saxon parameters

$$\beta_{2\text{U,WS}} \approx 0.28, \quad \gamma_{\text{U}} \lesssim 17^\circ$$



Low-energy estimate with rigid rotor assumption from B(E2) data

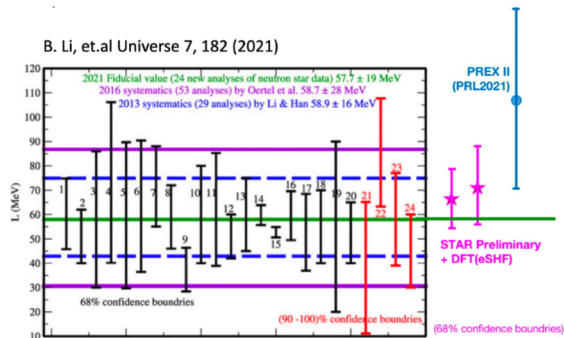
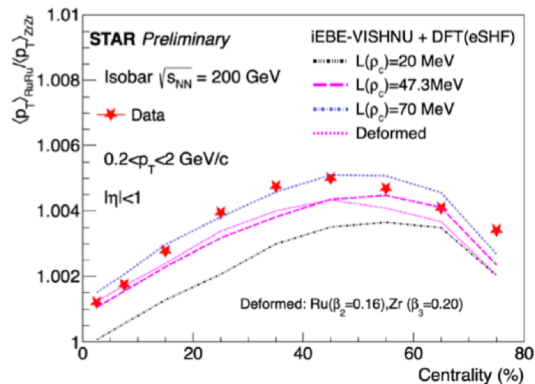
$$\beta_{2,\text{LD}} = \frac{4\pi}{5R_0^2 Z} \sqrt{\frac{B(\text{E}2)}{e^2}}$$

$$\beta_{2\text{U,LD}} = 0.287 \pm 0.007 \quad \gamma_{\text{U,LD}} = 6^\circ - 8^\circ \quad 1312.5975 \text{ PRC54, 2356 (1996)}$$

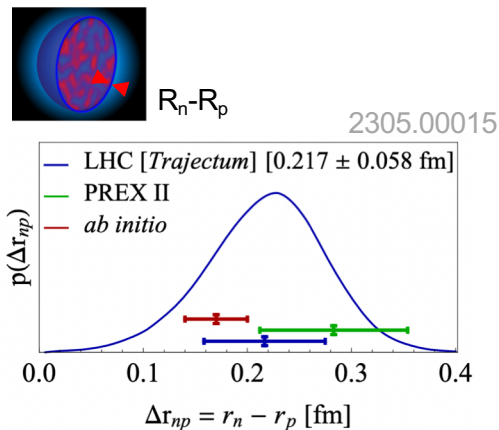
Imaging the radial structures

See talks by Haojie and Chunjian

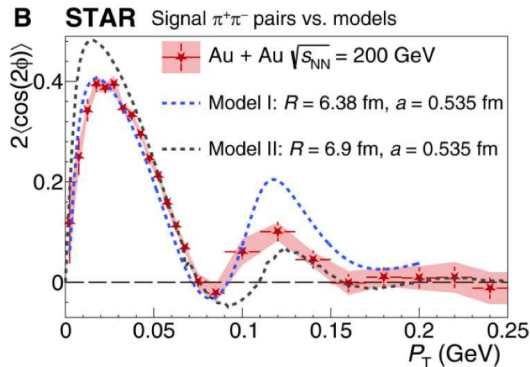
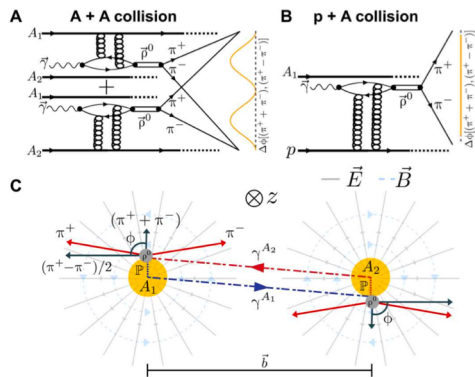
Radial parameters R_0 , a_0 are properties of one-body distribution, constrained by $\langle p_T \rangle$, $\langle N_{ch} \rangle$, σ_{tot} , $v_2^{RP} \sim v_2 \{4\}$



Constrain neutron skin and symmetry energy



Also accessed via photo-nuclear diffractive process in UPC or e+A

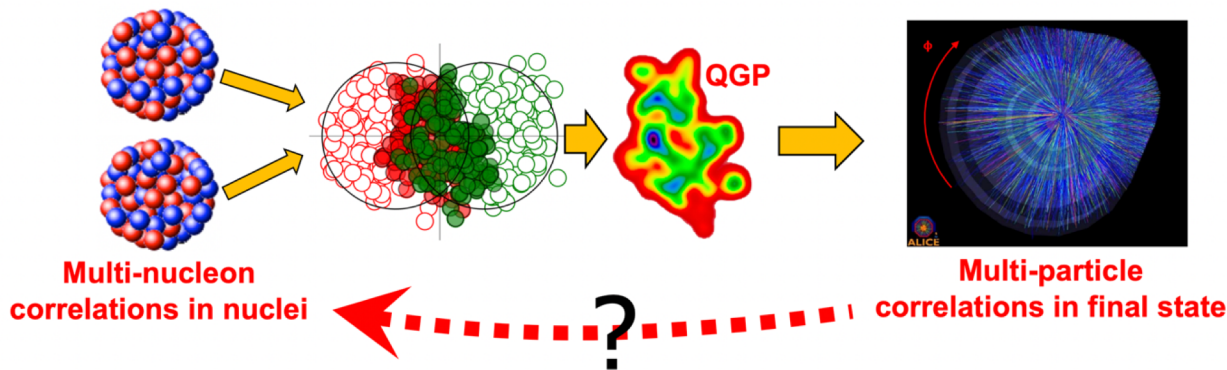


$$\Delta R_{Au} = R_n - R_p = 0.17 \pm 0.03 \text{ (stat.)} \pm 0.08 \text{ (sys.) fm}$$

$$\Delta R_U = R_n - R_p = 0.44 \pm 0.05 \text{ (stat.)} \pm 0.08 \text{ (sys.) fm}$$

Science Advance 9, 3903 (2023)

Opportunities at the intersection of nuclear structure and hot QCD



Many examples in <https://arxiv.org/abs/2209.11042>, but here is my list

- Probe octupole and hexadecapole deformations via v_3 and v_4 in central collisions.
- Gauge shape of odd-mass nuclei by comparing with neighboring even-even nuclei.
- Separate average shape from shape fluctuations via multi-particle correlations
- Constrain the radial structure of nuclei, including the neutron skin
- Structure in small systems including alpha clustering (e.g. $^{16}\text{O}+^{16}\text{O}$ vs $^{20}\text{Ne}+^{20}\text{Ne}$)

.....

See recent [INT program 23-1A](#)

Summary and outlook

- High-energy collisions image nuclear shape at ultra-short time scale of 10^{-24} s; Large particle multiplicity enables many-particle correlation event-by-event to probe many-nucleon correlations in nuclei.
- Collisions of carefully-selected isobar species (at LHC) can reveal the many-body nucleon correlations & constrain the heavy ion initial condition from small to large nuclei

2102.08158

| A | isobars | A | isobars | A | isobars | A | isobars | A | isobars | A | isobars |
|----|-----------|-----|------------|-----|---------|-----|------------|-----|---------|-----|------------|
| 36 | Ar, S | 80 | Se, Kr | 106 | Pd, Cd | 124 | Sn, Te, Xe | 148 | Nd, Sm | 174 | Yb, Hf |
| 40 | Ca, Ar | 84 | Kr, Sr, Mo | 108 | Pd, Cd | 126 | Te, Xe | 150 | Nd, Sm | 176 | Yb, Lu, Hf |
| 46 | Ca, Ti | 86 | Kr, Sr | 110 | Pd, Cd | 128 | Te, Xe | 152 | Sm, Gd | 180 | Hf, W |
| 48 | Ca, Ti | 87 | Rb, Sr | 112 | Cd, Sn | 130 | Te, Xe, Ba | 154 | Sm, Gd | 184 | W, Os |
| 50 | Ti, V, Cr | 92 | Zr, Nb, Mo | 113 | Cd, In | 132 | Xe, Ba | 156 | Gd, Dy | 186 | W, Os |
| 54 | Cr, Fe | 94 | Zr, Mo | 114 | Cd, Sn | 134 | Xe, Ba | 158 | Gd, Dy | 187 | Re, Os |
| 64 | Ni, Zn | 96 | Zr, Mo, Ru | 115 | In, Sn | 136 | Xe, Ba, Ce | 160 | Gd, Dy | 190 | Os, Pt |
| 70 | Zn, Ge | 98 | Mo, Ru | 116 | Cd, Sn | 138 | Ba, La, Ce | 162 | Dy, Er | 192 | Os, Pt |
| 74 | Ge, Se | 100 | Mo, Ru | 120 | Sn, Te | 142 | Ce, Nd | 164 | Dy, Er | 196 | Pt, Hg |
| 76 | Ge, Se | 102 | Ru, Pd | 122 | Sn, Te | 144 | Nd, Sm | 168 | Er, Yb | 198 | Pt, Hg |
| 78 | Se, Kr | 104 | Ru, Pd | 123 | Sb, Te | 146 | Nd, Sm | 170 | Er, Yb | 204 | Hg, Pb |

